

The effect of magnetic nanoparticles on the morphology, ferroelectric, and magnetoelectric behaviors of CFO/P(VDF-TrFE) 0–3 nanocomposites

J. X. Zhang,^{a)} J. Y. Dai,^{b)} L. C. So, C. L. Sun, C. Y. Lo, S. W. Or, and H. L. W. Chan^{b)}

Department of Applied Physics, The Hong Kong Polytechnic University, Hung Hom, Kowloon, Hong Kong, People's Republic of China

(Received 10 October 2008; accepted 3 January 2009; published online 4 March 2009)

Multiferroic nanocomposite films composed of P(VDF-TrFE) copolymer and CoFe_2O_4 (CFO) nanoparticles have been prepared by a modified polymeric processing. Structural characterizations reveal that CFO nanoparticles with 80–100 nm diameters are well distributed in the P(VDF-TrFE) matrix. The crystalline and microstructure of P(VDF-TrFE) are strongly dependent on the volume fraction of CFO nanoparticles, which are further analyzed by Raman spectra. Consequently, the ferroelectric and magnetoelectric responses are strongly influenced by the concentration of CFO nanoparticles. A significant magnetoelectric coupling effect of around 40 mV/cm Oe is obtained from the nanocomposites. A relatively simple model has been adopted to calculate the magnetoelectric coefficient, which is also in agreement with the experimental results. © 2009 American Institute of Physics. [DOI: [10.1063/1.3078111](https://doi.org/10.1063/1.3078111)]

I. INTRODUCTION

In recent years, magnetoelectric (ME) nanocomposite materials composed of ferroelectric and magnetic materials are being rigorously studied owing to the fact that these materials can realize the conversion between magnetic energy and electric energy, and are the model systems for nanometer-scaled ME coupling mechanism study. Compared to the well-studied inorganic piezoelectric materials such as $\text{Pb}(\text{Zr}_x\text{Ti}_{1-x})\text{O}_3$ (PZT) and $\text{Pb}(\text{Mg}_{1/3}\text{Nb}_{2/3})\text{O}_3$ –30% PbTiO_3 (PMN-PT), the poly(vinylidene fluoride-trifluoroethylene) [P(VDF-TrFE)] copolymer has a relatively good voltage sensitivity, high electromechanical properties, low dielectric constant, and low dielectric loss. Moreover, polymeric piezoelectric materials can stand freely without the substrate clamping effect, which is the main issue for other thin-film structures, and their shapes and sizes can also be easily modified by conventional polymeric processing.

Calculation by double inclusion method shows that the size of nanoparticles influence the dielectric constant and the breakdown strength and it suggests that the particles size should be around 100 nm or smaller in order to take advantage of the effective exchange coupling.¹ Recently, the laminated and particulate ME composites such as terfenol-D/PZT (Ref. 2) and NiFe_2O_4 /PZT (Ref. 3) have shown large ME coefficients in experimental observations⁴ and theoretical calculations,⁵ but some investigations on ME nanocomposite films such as CoFe_2O_4 / BaTiO_3 (Ref. 6) and BiFeO_3 / NiFe_2O_4 (Ref. 7) thin-film heterostructures and CFO/PZT (Ref. 8) 0–3 composite thin films, PZT/ferrite (Ref. 9) multilayered thin films have also been carried out since they may have potential applications in microelectromechanical system (MEMS).

Many studies on ceramic/polymer composites, such as

PT/P(VDF-TrFE),¹⁰ PZT/P(VDF-TrFE),¹¹ and even Ni/P(VDF-TrFE) (Ref. 12) nanocable structures, concerned mainly the dielectric and ferroelectric properties of the composite films. Only some reports focus on the ME properties of the polymer/alloy-based and metal/ceramic based 0–3 composites; however, due to the large leakage current and easy oxidization, the alloy-based magnetostrictive materials, to some extent, have limitations when used in nanocomposite, especially for thin film structure. As a replacement, oxide based magnetostrictive materials have been proposed for application in ME nanocomposites. Among different magnetic oxide materials, CoFe_2O_4 (CFO) has almost the largest magnetostrictive coefficients ($\lambda_s = -110 \times 10^{-6}$ at 300 K) with high Curie temperature (above 700 K). It is also an economic alternative to the existing alloy-based magnetostrictive materials. In this paper, we report CFO/P(VDF-TrFE) 0–3 nanocomposite films with good ferroelectric, magnetic, and ME response at room temperature. The concentration of CFO nanoparticles significantly influences the structure and properties of the copolymer matrix. The calculated result of the ME coefficient is also in good agreement with our experimental observation.

II. EXPERIMENT

The CFO nanoparticles were synthesized by a sol-gel process. Stoichiometric quantities of $\text{Co}(\text{CH}_3\text{CO}_2)_2 \cdot 4\text{H}_2\text{O}$ (0.01 mol) and $\text{Fe}(\text{NO}_3)_3 \cdot 9\text{H}_2\text{O}$ (0.02 mol) were first dissolved in a solution containing citric acid (0.02 mol) and ethylene glycol (40 ml) and stirred continuously at 70 °C for 2 h. A transparent sol solution was formed after 24 h aging. The nanoparticles were formed after postannealing under air ambient conditions in a tube furnace. We carefully study the annealing conditions in order to control the formation of CFO nanopowders with a diameter of approximately 100 nm. After the evaporation of the organic elements from the sol solution at 400 °C and an annealing process at 600 °C for 2 h, the CFO nanopowders were formed. The prepared

^{a)}Electronic mail: 06900302r@polyu.edu.hk.

^{b)}Author to whom correspondence should be addressed. Electronic mail: apdaijy@inet.polyu.edu.hk; apahlcha@inet.polyu.edu.hk.

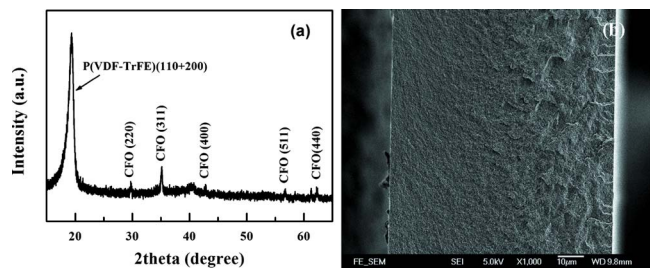


FIG. 1. (Color online) (a) XRD pattern of the CFO/P(VDF-TrFE) nanocomposite and (b) SEM image of the cross section of the nanocomposite with low magnification.

CFO nanopowders were dispersed in the P(VDF-TrFE) copolymer solution with a VDF/TrFE molar ratio of 70/30 in an ultrasonic bath for 2 h. The copolymer solution was prepared by dissolving P(VDF-TrFE) pellets, supplied by Pizotck Co., into methyl-ethyl-ketone (MEK). After vacuum and thermal treatment, the final crystallized CFO/P(VDF-TrFE) nanocomposite films with different CFO volume fractions were formed. The thickness of the nanocomposite films was controlled to $\sim 80 \mu\text{m}$ and the CFO volume fractions in the copolymer matrix were 8%, 23%, 37%, 48%, and 59%, determined by the equation $\rho = \Phi\rho_c + (1 - \Phi)\rho_p$, where Φ is the CFO volume fraction, and ρ , ρ_c , and ρ_p are the densities of the nanocomposite, the CFO nanopowders and the P(VDF-TrFE) matrix.

III. RESULTS AND DISCUSSIONS

The structural characterization of the composite films was carried out by x-ray diffraction (XRD) using a Bruker D8 Discover XRD system equipped with copper radiation. Figure 1(a) shows the typical XRD pattern of the composite films. It can be seen that all peaks can be identified as either the CFO nanoparticles or the P(VDF-TrFE) copolymer, where the sharp peak around 20° indicates the (110) and (200) atomic planes of P(VDF-TrFE) copolymer and all other peaks can be attributed to the CFO phase. This result suggests that the CFO nanoparticles embedded in P(VDF-TrFE) copolymer are polycrystalline and have no preferential crystallographic orientations. The microstructure of the nanocomposite films were studied by field emission scanning electron microscopy (SEM, JSM-6335F at 3.0 kV, JEOL, Tokyo, Japan). The cross-sectional SEM image with low magnification, shown in Fig. 1(b), confirms that the thickness of the free standing nanocomposite films is $\sim 80 \mu\text{m}$ and that there is no aggregation of the CFO nanoparticles.

Figures 2(a)–2(e) give the typical cross-sectional SEM images of the nanocomposite films with the volume fractions of 0, 8%, 37%, 48%, and 59% respectively. It can be observed that the pure P(VDF-TrFE) copolymer has a chainlike structure. With the addition of CFO nanoparticles, this chainlike structure disappears gradually, especially when the volume fraction of CFO nanoparticles reaches 48%. Therefore, the overall morphology of the nanocomposite is influenced by the particle loading dramatically: in the low particle loading state, the nanoparticles are embedded into the chainlike network, while in the heavy addition of particles, they tend to be wrapped by the whole copolymer matrix and the chain-

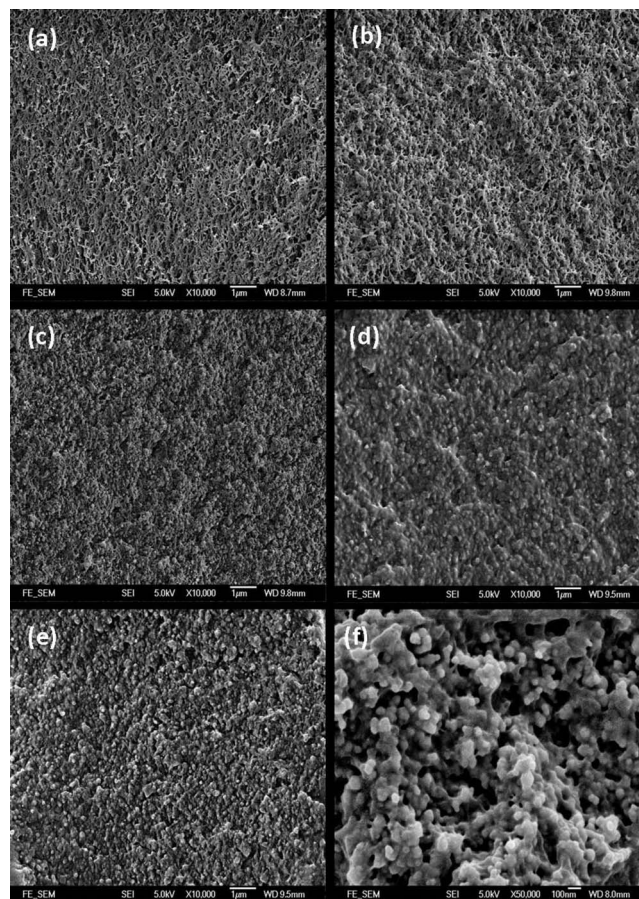


FIG. 2. [(a)–(e)] The cross-sectional SEM images of CFO/P(VDF-TrFE) nanocomposites with different CFO volume fractions, and (f) the SEM image of the nanocomposite with a CFO volume fraction of 48% after ICP treatment.

like structure of P(VDF-TrFE) disappears. Figure 1(f) shows the SEM image of the nanocomposites with a volume fraction of 48% after inductor coupled plasma (ICP) treatment. It is evident that the CFO nanoparticles with sizes of 80–100 nm are dispersed uniformly without serious agglomeration in the copolymer matrix. The good compatibility between CFO and P(VDF-TrFE), especially in the 0–3 composite structure, can result in excellent mechanical, dielectric properties, and ME coupling properties.

The volume fraction-dependent Raman spectra of the CFO/P(VDF-TrFE) nanocomposite are given in Fig. 3. The band around 889 and 848 cm^{-1} indicate the symmetric CF_2 stretching mode of the crystalline beta phase. The band around 803 cm^{-1} is associated with the symmetric CF_2 stretching modes of the α phase.¹³ We can observe that the intensity of the trans band at 889 and 848 cm^{-1} decreases with the loading of CFO nanoparticles and disappears when the volume fraction of CFO reaches 59%. Since the ferroelectric property occurs in the crystalline beta phase that consists of polymer chains, arranged in a pseudohexagonal lattice (space group $m2m$), the addition of CFO magnetic nanoparticles may induce the change in microstructure of the copolymer and can further reduce the content of ferroelectric phase in P(VDF-TrFE). The nanoparticle doping-induced change in crystalline structure can also be found in ferrite/PVDF nanocomposite fibers, which is reported elsewhere.¹⁴

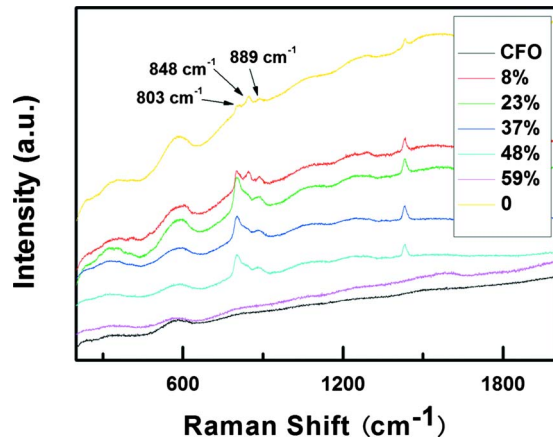


FIG. 3. (Color online) Raman spectra of CFO/P(VDF-TrFE) nanocomposites with different volume fractions of CFO nanoparticles.

For the ferroelectric property measurement, Au electrodes with 3 mm diameter were deposited by magnetron sputtering. The ferroelectric hysteresis loops of the CFO/P(VDF-TrFE) nanocomposites were measured by using a standard Sawyer–Tower circuit at 10 Hz. As shown in Fig. 4(a), well-defined ferroelectric hysteresis loops were obtained when the applied electric field is strong enough. Tested under a field with a maximum strength of 150 MV/m, all of the samples were found to exhibit saturated hysteresis loops with remnant polarizations (P_r) of 10.7, 6.3, 6.3, 5.8, and 5.9 $\mu\text{C}/\text{cm}^2$, for the samples with volume fractions of 0, 8%, 23%, 37%, and 48% respectively; a value of 2.9 $\mu\text{C}/\text{cm}^2$ was measured for the sample with a volume fraction of 59%. We can also find that the coercive field (E_c) is strongly dependent on the volume fraction of CFO nanoparticles and changes from 58.6 to 34.3, 41.5, 44.1, 40.8 and 31.3 MV/m under different CFO volume fractions. The overall remnant polarizations of pure copolymer and the nanocomposites with low CFO addition are much larger than that of P(VDF-TrFE) thin films (3.1 $\mu\text{C}/\text{cm}^2$).¹⁵ After corona poling at room temperature, the piezoelectric coefficients (d_{33}) were measured to be 24.4, 14.9, 18.1, 18.6, 17.7, and 8.5 pC/N, for the samples with volume fractions of 0, 8%, 23%, 37%, 48%, and 59%, respectively. The addition of low dielectric constant CFO nanoparticles does not reduce the dielectric constant of the P(VDF-TrFE) copolymer (the graph is not shown). The good dielectric and ferroelectric properties of the composite films can be attributed to the uniform dispersion of CFO nanoparticles without serious agglomeration in the P(VDF-TrFE) copolymer matrix when the loading of CFO is small. However, when the concentration of CFO nanoparticles reaches 59%, the value of remnant polarization and piezoelectric coefficient of the nanocomposite decreases dramatically. The addition of CFO nanoparticles in the sample with a volume fraction of 59% significantly influence the structure of the P(VDF-TrFE) matrix, as shown in the SEM images in Fig. 2 and the inset of Fig. 4(b), leading to the interruption of the charge transportation in copolymer during electrical measurement. This result is also in good agreement with the above Raman spectra analysis.

The magnetic hysteresis loop at room temperature was measured by a vibrating sample magnetometer (Lakeshore,

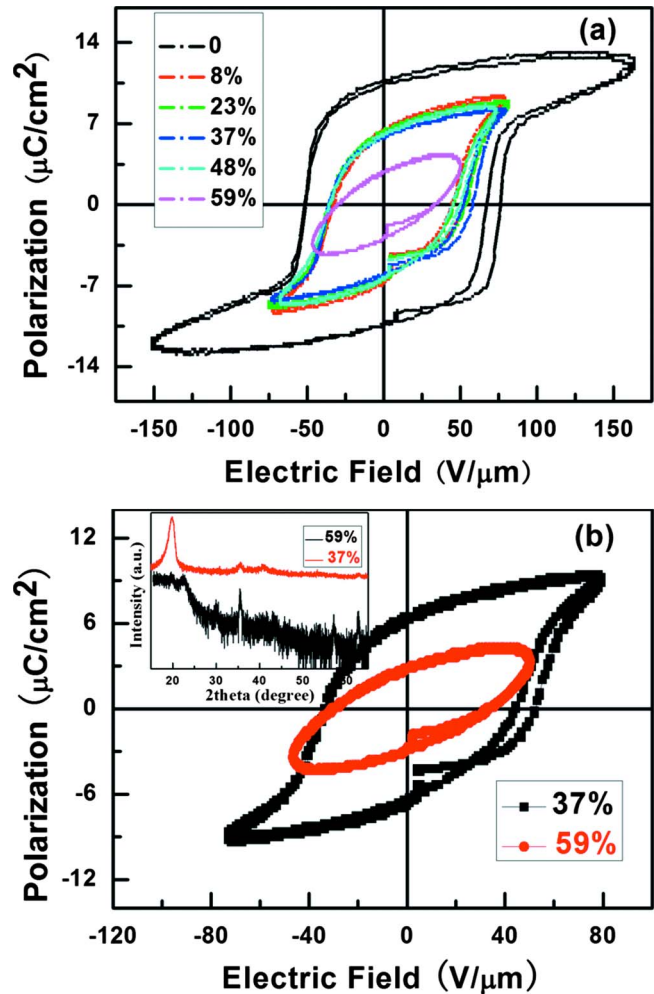


FIG. 4. (Color online) (a) Volume fraction-dependent ferroelectric hysteresis loops of CFO/P(VDF-TrFE) nanocomposites and (b) ferroelectric hysteresis loops of nanocomposites with the volume fractions of 37% and 59%. The inset in (b) is the corresponding XRD data.

Model 7300 series) with the applied field perpendicular to the surface of the composite films. Figure 5 shows the room temperature magnetic hysteresis curves of the samples with the measurement up to a field of 10 kOe. Saturated magnetization value reaches 50 emu/g which is comparable to that of CFO nanoparticles prepared by other methods.^{16,17} The

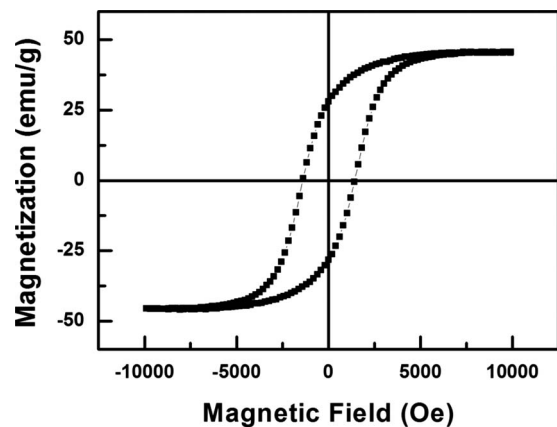


FIG. 5. Magnetization hysteresis loop for the CFO/P(VDF-TrFE) nanocomposites.

coercive field is 1400 Oe, similar to that of CFO nanowires measured at room temperature¹⁸ but is much lower than the value of CFO nanoparticles with the same size (coercive field reaches 5100 Oe).¹⁹ In particular, the nanoparticles in copolymer matrix possess a high remanence ratio of 66%, which is larger than the value reported before.¹⁹ The relatively large values of remanence ratio of the magnetically isotropic samples will enhance the ME response during mechanical coupling.

Prior to the measurement of the ME coupling response of the CFO/P(VDF-TrFE) copolymer nanocomposite, we first give a quantitative evaluation of the ME coupling effect. We adopted Wong and Shin's model^{20,21} to calculate the ME coefficient (α_E) of the nanocomposites as a function of magnetic bias field (Fig. 6). According to Shin's theory, the α_{E33} can be expressed by the equation

$$\alpha_{E33} = (1 - \phi) \frac{L_E}{\varepsilon} \left(d_{31m} \frac{dT_{xm}}{dH_p} + d_{32m} \frac{dT_{ym}}{dH_p} + d_{33m} \frac{dT_{zm}}{dH_p} \right) \times \left(\frac{dH_p}{dH} \right), \quad (1)$$

where $L_E = [\varepsilon_p + 2\varepsilon_m] / [(1 - \phi)\varepsilon_p + (2 + \phi)\varepsilon_m]$; m and p indicate the P(VDF-TrFE) copolymer matrix and the CFO nanoparticles; d_{31} , d_{32} , d_{33} , and ε are the piezoelectric coefficients and the dielectric constant; ϕ represents the volume fraction; T and H are the stress and applied magnetic field, respectively. We can derive T by solving the following elasticity equations (2) and boundary conditions (3) and (5):

$$\begin{aligned} e_{xp} &= T_{xp}/Y_p - \nu_p(T_{yp} + T_{zp})/Y_p + \lambda_{xp}(H_i), \\ e_{yp} &= T_{yp}/Y_p - \nu_p(T_{xp} + T_{zp})/Y_p + \lambda_{yp}(H_i), \\ e_{zp} &= T_{zp}/Y_p - \nu_p(T_{xp} + T_{yp})/Y_p + \lambda_{zp}(H_i), \\ e_{xm} &= T_{xm}/Y_m - \nu_m(T_{ym} + T_{zm})/Y_m, \\ e_{ym} &= T_{ym}/Y_m - \nu_m(T_{xm} + T_{zm})/Y_m, \\ e_{zm} &= T_{zm}/Y_m - \nu_m(T_{xm} + T_{ym})/Y_m, \end{aligned} \quad (2)$$

$$\begin{pmatrix} T_{xp} - T_{xm} \\ T_{yp} - T_{ym} \\ T_{zp} - T_{zm} \end{pmatrix} = \begin{pmatrix} A & B & B \\ B & A & B \\ B & B & A \end{pmatrix} \begin{pmatrix} e_{xp} - e_{xm} \\ e_{yp} - e_{ym} \\ e_{zp} - e_{zm} \end{pmatrix}, \quad (3)$$

where $A = 10\mu_m[2\mu_m/(k_m + 2\mu_m) - 3]/9$ and $B = -\mu_m[10\mu_m/(k_m + 2\mu_m) + 3]/9$, and k and μ denote the bulk modulus and shear modulus. According to Duenas's model, the magnetostrictive coefficient (λ) can be expressed by the equation

$$\lambda_p = \lambda_{\text{sat},p} \tanh^2(3\chi_p H_p / M_{\text{sat},p}). \quad (4)$$

Since our sample is not clamped in the x , y , or z directions, the overall stress can be represented by the following:

$$T_l = \phi T_{pl} + (1 - \phi) T_{ml} = 0. \quad (5)$$

dH_p/dH can be calculated by the equation

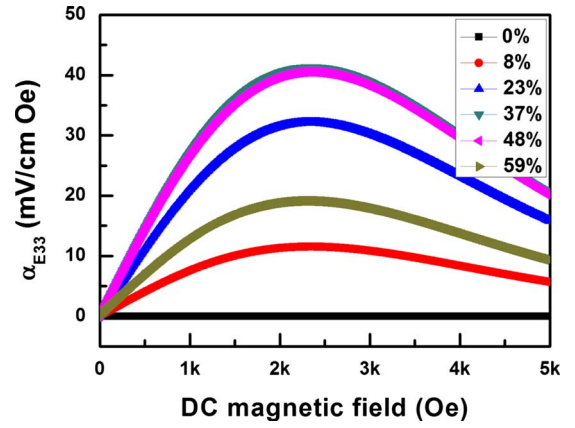


FIG. 6. (Color online) Theoretical calculation of the ME coefficient as a function of dc magnetic bias field for the CFO/P(VDF-TrFE) nanocomposites with different volume fractions.

$$\frac{dH_p}{dH} = \frac{3\xi_m}{(1 - \phi)(\xi_p + dM_p/dH_p) + (2 + \phi)\xi_m}, \quad (6)$$

where ξ and M are the magnetic permeability and magnetization. We can obtain dM_p/dH_p by the M - H loop (Fig. 5) and Duenas's model [$M_p = M_{\text{sat},p} \tanh(3\chi_p H_p / M_{\text{sat},p})$]. Therefore, α_E is determined by Eqs. (2)–(6). The parameters of the constituents adopted for the calculations can be found in our measured data and elsewhere.^{21,22} Figure 6 shows the theoretical calculation of the bias magnetic field-dependent ME coefficient of CFO/P(VDF-TrFE) nanocomposite films with different volume fractions. Evidently, the largest ME coefficient appears at a magnetic bias field of around 2 kOe in the sample with a CFO nanoparticle volume fraction of 37%. When the volume fraction further increases, the ME coefficient decreases. The material parameters used in this calculation is shown in Table I. The piezoelectric constant of the P(VDF-TrFE) is provided in the section of ferroelectric discussion.

The ME voltage coefficient of the nanocomposite film was measured in transverse mode by a dynamic measurement setup. We measured the electric field produced by an alternating magnetic field applied to the nanocomposite. A small alternative current (ac) magnetic field H_3 (with an amplitude of 1 Oe and a frequency of 5 kHz) was in parallel and superimposed on a direct current (dc) bias field (range from 0 to 5 kOe) to activate the dynamic magnetostriction of the CFO nanoparticles embedded in the P(VDF-TrFE) copolymer. The H_3 was provided by a Helmholtz coil driven by the dynamic signal analyzer via the constant-current-supply amplifier, and the H_{bias} was controlled by the dc power supply,

TABLE I. Material parameters (dielectric constant ε , permeability ξ , Young's modulus Y , shear modulus μ , Poisson ration ν , bulk modulus k , piezoelectric coefficient d , susceptibility χ , magnetostrictive λ , and magnetostrictive strain ratio β) for P(VDF-TrFE) and CFO used for theoretical values.

Material	ε	ξ	Y (GPa)	μ (GPa)	ν	K (GPa)	χ	λ	β
P(VDF-TrFE)	11	1	153	0.5	0.39	197			
CFO	10	2	1.39	56	0.37	2.16	0.03	10^{-4}	0.5

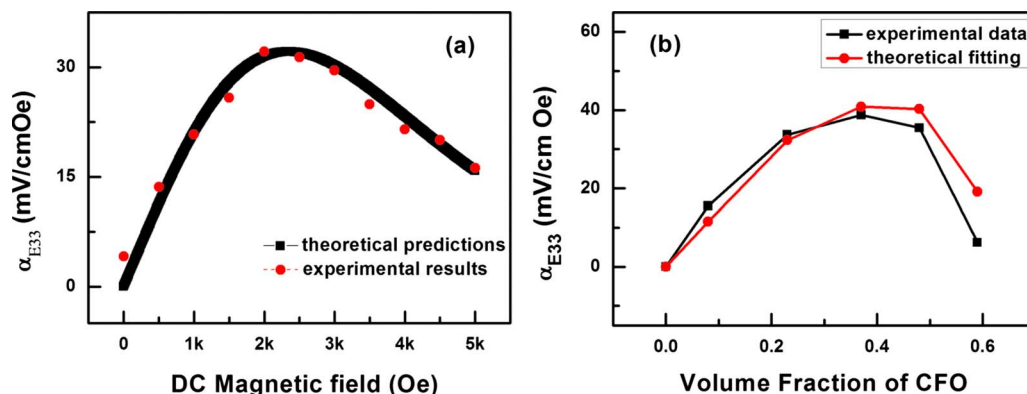


FIG. 7. (Color online) ME coefficients of CFO/P(VDF-TrFE) nanocomposite with a volume fraction of 23% and (b) ME coefficients of nanocomposite with different CFO volume fractions at a dc magnetic bias field of 2 kOe.

where H_3 and H_{bias} were simultaneously applied and monitored by a gaussmeter. The voltage generated by the input magnetic field was recorded by a multipurpose fast Fourier transform analyzer (CF-5200).

Figure 7(a) gives the calculated ME voltage coefficient and the experimental values as a function of dc magnetic bias field under an ac magnetic field of 5 kHz. Without substrate clamping effect during the vibration of the magnetostrictive and the piezoelectric phases, significant magnetic induced voltage response in the CFO/P(VDF-TrFE) nanoparticles system is observed. With the increase in the dc magnetic bias field, the ME effect increases and reaches the maximum value at a bias field of 2 kOe; the α_E then decreases slowly as the dc magnetic bias field further increases. The nonlinear ME response is closely related to the magnetostrictive behavior of the CFO nanoparticles. The initial increase in ME output can be attributed to the enhancement of the domain wall movement and the rotation in CFO nanoparticles, which facilitates the magnetostriction in the CFO phase. When the bias field approaches 2 kOe, the magnetic induced strain in CFO nanoparticles begins to reach saturation. As a result, beyond a bias field of 2 kOe, the output voltage in the piezoelectric materials generated from the elastic interaction between the two phases decreases, and the ME output decreases slightly. Figure 7(b) shows the ME coefficient at a bias field of 2 kOe of the samples with different volume fractions of CFO nanoparticles. The theoretical fitting is also provided. The slightly discrepancy between the experimental data and the theoretical evaluation may be due to the reason that the good dispersion of low resistance CFO nanoparticles cannot be remained in the samples with high volume fractions, leading to the interruption of microstructure and ferroelectric properties of the nanocomposites.

IV. CONCLUSION

We have observed significant ME coupling effect in the CFO/P(VDF-TrFE) copolymer 0–3 nanocomposites films. The volume fraction-dependent microstructure and ferroelectric properties of the composite films were studied extensively. The microstructure of P(VDF-TrFE) can be influenced by the addition of CFO nanoparticles. The low dielectric constant CFO does not significantly reduce the piezoelectric coefficient, dielectric constant, and the remnant

polarization of the P(VDF-TrFE) copolymer when the concentration of CFO nanoparticles is below 59%. The ME voltage coefficient results show that the ME effect of the nanocomposite film is highly dependent on the volume fraction and the dc magnetic bias. A relatively simple method was used to evaluate the theoretical ME coefficient in the nanocomposite. Experimental observation of ME coefficient is in agreement with our calculated predictions.

ACKNOWLEDGMENTS

The authors would like to thank the financial support from the collaboration project grant between the Hong Kong Polytechnic University and Beijing Institute of Technology (No. 1-BB84). J. Y. Dai is grateful to the financial support from the Hong Kong GRF grant: PolyU 5005/08P. The authors gratefully acknowledge discussions with Dr. C. K. Wong and Prof. F. G. Shin (Dept. of Appl. Phys, The Hong Kong PolyU).

- ¹J. Y. Li, L. Zhang, and S. Ducharme, *Appl. Phys. Lett.* **90**, 132901 (2007).
- ²S. Dong, J. Zhai, J. F. Li, D. Viehland, and M. I. Bichurin, *Appl. Phys. Lett.* **89**, 243512 (2006).
- ³G. Srinivasan, E. T. Rasmussen, J. Gallegos, R. Srinivasan, Yu. I. Bokhan, and V. M. Laletin, *Phys. Rev. B* **64**, 214408 (2001).
- ⁴C.-W. Nan, N. Cai, Z. Shi, J. Zhai, G. Liu, and Y. Lin, *Phys. Rev. B* **71**, 014102 (2005).
- ⁵C. W. Nan, M. Li, and J. H. Huang, *Phys. Rev. B* **63**, 144415 (2001).
- ⁶H. Zheng, J. Wang, S. E. Lofland, Z. Ma, L. Mohaddes-Ardabili, T. Zhao, L. Salamanca-Riba, S. R. Shinde, S. B. Ogale, F. Bai, D. Viehland, Y. Jia, D. G. Schlom, M. Wuttig, A. Roytburd, and R. Ramesh, *Science* **303**, 661 (2004).
- ⁷Q. Zhan, R. Yu, S. P. Crane, H. Zheng, C. Kisielowski, and R. Ramesh, *Appl. Phys. Lett.* **89**, 172902 (2006).
- ⁸J.-G. Wan, H. Zhang, X. Wang, D. Pan, J.-M. Liu, and G. Wang, *Appl. Phys. Lett.* **89**, 122914 (2006); J. X. Zhang, J. Y. Dai, W. Lu, H. L. W. Chan, B. Wu, and D. X. Li, *J. Phys. D* **41**, 235405 (2008).
- ⁹H.-C. He, J. Wang, J.-P. Zhou, and C.-W. Nan, *Adv. Funct. Mater.* **17**, 1333 (2007); J. X. Zhang, J. Y. Dai, C. K. Chow, C. L. Sun, V. C. Lo, and H. L. W. Chan, *Appl. Phys. Lett.* **92**, 022901 (2008).
- ¹⁰Y. Yang, H. L. W. Chan, and C. L. Choy, *Integr. Ferroelectr.* **69**, 239 (2005).
- ¹¹H. L. W. Chan, P. K. L. Ng, and C. L. Choy, *Appl. Phys. Lett.* **74**, 20 (1999).
- ¹²C.-L. Sun, K. H. Lam, C. Chao, S. T. Lau, and H. L. W. Chan, *Appl. Phys. Lett.* **90**, 253107 (2007).
- ¹³K. Tashiro, H. Kaito, and M. Kobayashi, *Polymer* **33**, 14 (1992).
- ¹⁴J. S. Andrew and D. R. Clarke, *Langmuir* **24**, 8435 (2008).
- ¹⁵J. J. Li, Y. Neo, H. Mimura, K. Omote, and K. Yokoo, *Appl. Phys. Lett.* **89**, 222907 (2006).

- ¹⁶P. Jeppson, R. Sailer, E. Jarabek, J. Sandstrom, B. Anderson, M. Bremer, D. G. Grier, D. L. Schulz, A. N. Caruso, S. A. Payne, P. Eames, M. Tondra, H. He, and D. B. Chrisey, *J. Appl. Phys.* **100**, 114324 (2006).
- ¹⁷P. P. Vaishnava, U. Senaratne, E. Buc, and R. Naik, V. M. Naika, G. Tsoi, L. E. Wenger, and P. Boolchand, *J. Appl. Phys.* **99**, 08G702 (2006).
- ¹⁸Z. T. Zhang, A. J. Rondinone, J.-X. Ma, J. Shen, and S. Dai, *Adv. Mater.* (Weinheim, Ger.) **17**, 1415 (2005).
- ¹⁹B. H. Liu and J. Ding, *Appl. Phys. Lett.* **88**, 042506 (2006).
- ²⁰C. K. Wong and F. G. Shin, *J. Appl. Phys.* **102**, 063908 (2007).
- ²¹Y. Zhou and F. G. Shin, *J. Appl. Phys.* **100**, 043910 (2006).
- ²²M. I. Bichurin, V. M. Petrov, and G. Srinivasan, *Phys. Rev. B* **68**, 054402 (2003).